EFFECTS OF STRUCTURE AND COMPOSITION

OF LEAD GLASSES ON

THERMAL LENSING

By

BAHMAN TAHERI

Bachelor of Science

California Polytechnic State University
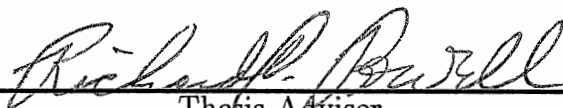
San Luis Obispo, California

1989

Submitted to the Faculty of the
Graduate College of the
Oklahoma State University
in partial fulfillment of
the requirements for
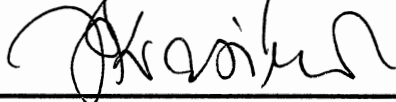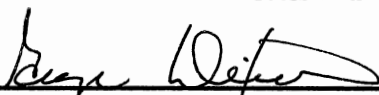the Degree of
MASTER OF SCIENCE
July, 1992

Shears
1992
T128e

EFFECTS OF STRUCTURE AND COMPOSITION

OF LEAD GLASSES ON

THERMAL LENSING

Thesis Approved:

_____
Thesis Adviser

_____

_____

_____
Dean of the Graduate College

ACKNOWLEDGMENTS

The organization and thought process taught to individuals in a graduate program is as important as the subject matter studied. This section is thus devoted to acknowledging the people who have educated me in these areas both inside and outside the realms of physics.

I wish to express my gratitude to Dr. R. C. Powell for giving me the opportunity to work in his lab. From him I have learned thought process and organization as well as material science. His encouragement to try different ideas have proved immeasurable. Also gratitude is extended to my other committee members Dr. G. S. Dixon and Dr. J. S. Krasinski for their time and patience.

To Dr.s Antonio Munoz, Baha Jassemnejad and Roger Reeves with all of whom I have had many insightful discussions. Their knowledge and enthusiasm has helped me understand numerous physical concepts. In particular Dr. Munoz played an immeasurable role in completion of the work presented.

To my fellow graduate students, Doyle St. John, Roger Petrin and Keith Ver Steeg for laboratory assistance.

To Mrs. Carol Wicksted who has patiently taught me organization. Her friendly smile and reassurance has helped me overcome many stressful situations.

Finally, my parents Fereidoun and Mehry, from whom I learned the most. My father's belief in higher education along with my mother's belief in me, have eased the most difficult decisions of my life. For their love and support I thank them.

TABLE OF CONTENTS

LIST OF TABLES

v

LIST OF FIGURES

CHAPTER I

INTRODUCTION

In the past decade there has been significant interest in characterizing the transmission properties of laser beams in glass for applications to systems used in optical technology. With high laser powers, the nonlinear optical properties of the material become important. These can be characterized by the macroscopic polarizability, P, of the material due to an electric field via the susceptibility tensor,

$$P = \chi^{(1)}\mathbf{E} + \chi^{(2)}\mathbf{EE} + \chi^{(3)}\mathbf{EEE} + \dots \tag{1}$$

where $\chi^{(n)}$ is the susceptibility tensor of rank $n + 1$. Nonlinear optical behavior is attributed to susceptibilities of order greater than $\chi^{(1)}$. Glasses are centrosymmetric materials and thus their dominant nonlinear optical effects are associated with $\chi^{(3)}$. For a linearly polarized laser beam of intensity I and frequency ω incident on the sample, this will manifest itself in an intensity dependent change in the refractive index represented by

$$\Delta n = \gamma I = \frac{480\pi^2}{cn_0^2}\chi^{(3)}(-\omega,\omega,\omega,-\omega) \tag{2}$$

where γ is the nonlinear refractive coefficient with contributions from Kerr, electrostrictive and thermal effects. It has been shown that in glasses under illumination of nanosecond duration laser pulses, the main contributions to γ arise from Kerr and thermal effects[1]. Further, as shown in chapt. II of this thesis, the strength of the thermal contribution of γ is dependent on the absorption coefficient of the material. Due to the relatively high absorption coefficients of the glasses under study here, the main contribution to γ is thermal. The change in the

1

refractive index caused by the thermal contributions to γ can lead to a physical effect referred to as thermal lensing which is the focus of this thesis.

Qualitatively, thermal lensing arises when an optical beam passes through a medium of finite absorption in which some of the absorbed energy is converted into heat. The local change in the temperature results in a change in the optical path length, (nL), of the medium with a radial profile determined by the laser beam induced temperature profile. Such a change in (nL) will cause the material to act as a lens which leads to a focusing or defocusing of the input beam, depending on the radial profile of the (nL) change. The relevant time scale for this effect is determined by the time of heat propagation across the beam,[1,2]. During nanosecond excitation, thermal conduction is not significant and local heating of the medium occurs.[3]

Thermal lensing can alter the output of a laser system operating in a continuous mode and thus has been the focus of much theoretical[2,4-7] and experimental[8-14] work. Recent use of thermal lensing effects in some optical devices[15,16] in the nanosecond regime has renewed interest in studying the thermal lensing characteristics of glasses under laser pulses in this time scale. These studies take the form of determination of the thermo-optic coefficient, dn/dT, of materials via three wave mixing and interferometric techniques. Single beam determination of dn/dT has allowed investigation of the device applications to take place while investigating the physical nature of the processes of thermal lensing.

Summary of Thesis

The work presented here is a summary of the results of fluence transmission experiments using a tight focus geometry, with a 7 ns pulsed laser at 457 nm, performed on several glasses. Table I shows the composition of the glasses studied. Emphasis was placed on lead glasses which were found to exhibit the greatest thermal lensing effects in the geometry used. Results of a systematic study of the thermal lensing characteristics of several different types of lead glasses are reported

TABLE I

COMPOSTION OF GLASS SAMPLES

Glass	Composition (mol %)	Thickness (mm)	Glass	Composition (mol %)	Thickness (mm)
LB1	60.0 B_2O_3 15.0 Li_2O 20.0 BaO 5.0 Eu_2O_3	3.20	LBGe	40.0 B_2O_3 27.7 GeO_2 24.0 PbO 3.3 BaO 5.0 Eu_2O_3	1.90
LB2	60.0 B_2O_3 15.0 Li_2O 20.0 MgO 5.0 Eu_2O_3	2.10	LG	67.7 GeO_2 24.0 PbO 3.3 BaO 5.0 Eu_2O_3	3.15
LB3	60.0 B_2O 15.0 Li_2O 20.0 CaO 5.0 Eu_2O_3	3.00	LS1	57.7 SiO_2 34.0 PbO 3.3 BaO 5.0 Eu_2O_3	1.00
LB4	60.0 B_2O_3 15.0 Li_2O 20.0 ZnO 5.0 Eu_2O_3	2.35	LS2	67.7 SiO_2 24.0 PbO 3.3 BaO 5.0 Eu_2O_3	1.95
LB5	60.0 B_2O_3 15.0 Li_2O 20.0 Al_2O_3 5.0 Eu_2O_3	0.90	MgS1	65.0 SiO_2 15.0 MgO 15.0 Na_2O 5.0 Eu_2O_3	5.15
LB6	60.0 B_2O_3 15.0 Li_2O 20.0 PbO 5.0 Eu_2O_3	1.60	MgS2	48.0 SiO_2 24.0 MgO 19.0 Al_2O_3 4.0 Ta_2O_5 5.0 Eu_2O_3	3.00
LB	67.7 B_2O_3 24.0 PbO 3.3 BaO	2.05	LP	67.7 P_2O_5 24.0 PbO 3.3 BaO	3.05

here. The effects of the network former ions, network modifier ions, and lead concentration on the thermal lensing characteristics of the glasses are determined.

Chapter II presents the theoretical aspects of these experiments. The thermal change in the refractive index is utilized and a model is developed based on geometric optics. This is used to determine the effects of the experimental parameters on the optical limiting characteristics of the glasses studied. It was found that the position of the sample, the sign and magnitude of the thermo-optic coefficient, density and the specific heat capacity of the material are among the parameters having the greatest influence on the results obtained.

In chapter III, the experimental aspects of the optical limiting characteristics of the samples are presented. Effects of geometric and material parameters on the thermal lensing characteristics of the glasses studied were investigated. The results show that glasses with a random network structure display greater thermal lensing than the ring or chain structures.

In chapter IV the experimental and theoretical results of the previous chapters are used to determine the best suited materials for thermal lensing. Finally, chapter V outlines some applications of the study presented here.

CHAPTER II

THEORETICAL

Background

Self modulation of a laser beam through a medium can occur through Kerr, electrorestictive or thermal effects. The strength of each process depends on material parameters such as density and bonding. In the following the result of such a modulation by thermal effects is considered.

A change in the temperature profile can be observed when a material is illuminated by a laser beam, dependent on the heat absorbed. Following the development in ref. 5, for a laser operating in the TEM_{00} mode with a Gaussian intensity profile given by

$$I(r,t) = \frac{2P(t)}{\pi\omega^2}e^{-\frac{2r^2}{\omega^2}} \tag{1}$$

where $P(t)$ is the instantaneous power, ω the beam waist, and r the radial distance from the optic axis, the resulting heat generated per unit length between r and $r + dr$ in the sample is given by

$$Q\,dr = \frac{4\alpha}{\omega^2}e^{-\frac{2r^2}{\omega^2}}H(t)r\,dr \tag{2}$$

where

$$H(t) = \int_0^t P(t)\,dt \tag{3}$$

To gain insight into the role of the time dependence, the temperature profile after the passage of the beam through the sample is first calculated. Since the pulse duration is in nanoseconds and relaxation processes in glasses are in microseconds, it is reasonable to assume that the heat generation occurs instantaneously. The Green's function for a two dimensional heat equation

$$D\nabla^2\Psi - \frac{\partial\Psi}{\partial T} = -4\pi D\rho \tag{4}$$

with instantanous heat generation is given by:

$$G(r,t) = \frac{1}{4\pi kt}I_0\left(\frac{rr'}{2Dt}\right)e^{-\frac{r^2+r'^2}{4Dt}} \tag{5}$$

where I_0 is the modified, zeroth order Bessel function, k is the thermal conductivity, ρ is the density and c is the specific heat capacity of the medium. The change in the temperature is

$$\Delta T(r,t) = \int G(r,t;r')Q(r')\,dr' \tag{6}$$

Using (4) and (7)

$$\Delta T(r,t) = \frac{2D\alpha H(t)}{\pi\omega^2 k(1+2t/t_c)}e^{-\frac{2r^2}{\omega^2(1+2t/t_c)}} \tag{7}$$

where

$$t_c = \omega^2/4D. \tag{8}$$

From the above, it is apparent that the temperature rise during the propagation of a 7 ns pulse, using $t/tc << 1$, can be approximated by

$$\Delta T = \frac{2D\alpha H(t)}{\pi\omega^2 k}e^{-\frac{2r^2}{\omega^2}} \tag{9}$$

Small changes in temperature result in a change in the optical path length given by[6,13]

$$\Delta(nL) = \left(\frac{dn}{dT} + (n-1)(1+\nu)\zeta\right)L\Delta T \tag{10}$$

where from temperature differentiation of the Lorentz-Lorenz equation,[10]

$$\frac{dn}{dT} = \frac{(n^2-1)(n^2+2)}{6n}(\Phi - 3\zeta) \tag{11}$$

where ν is Poisson's ratio and accounts for thermally induced "buldging", ζ the coefficient of linear expansion, L is the thickness of the material, and Φ is the change in the atomic polarizability. The first term in Eq. (10) accounts for changes

in the refractive index and the second for changes in the thickness due to thermal expansion of the material. The relative contribution of each term in Eqs. (10) and (11) is dependent on the material used and the time scale of the experiment. For example the response time of ζ be much longer than that of dn/dT. In the lead glasses studied here, typical values of 10^{-5} and 10^{-6} for dn/dT and ζ also suggests that the main contribution to changes in the optical path length is due to thermal changes in the index of refraction. On the other hand, the negative sign of the thermo-optic coefficient of some lead fluoride glasses indicates that the bulk expansion term in Eq. (11) plays a greater role than the polarizability term in determining dn/dT. With this in mind and to ease the mathematics, dn/dT is defined to incorporate both terms

$$\frac{dn}{dT} \equiv \left[\frac{dn}{dT} + (n-1)(1+\nu)\zeta \right] . \tag{12}$$

The change in the temperature will therefore result in a change in the refractive index

$$n = n_0 + \frac{dn}{dT}\Delta T \tag{13}$$

Substituting the expression in Eq. (11) for ΔT into Eq. (15), the change in the index of refraction can be written as

$$n(r,t) = \frac{2D\alpha H(t)}{\pi\omega^2 k}\frac{dn}{dT}e^{-\frac{2r^2}{\omega^2}} = \Delta n_0(t)e^{-\frac{2r^2}{\omega^2}} \tag{14}$$

From Eqs. (2) and (3), the change in the refractive index in terms of the nonlinear refractive coefficient is

$$\Delta n(r,t) = \gamma I(r,t) = \frac{2\gamma P(t)}{\pi\omega^2}e^{-\frac{2r^2}{\omega^2}} \tag{15}$$

By comparison of these two expressions for laser induced refractive index change, the nonlinear refractive coefficient, γ, and dn/dT can be related by

$$\gamma = \frac{dn}{dT}\frac{\alpha\tau}{\rho c} \tag{16}$$

where τ is the pulse width. This expression is used to estimate the values of the thermo-optic coefficients, dn/dT,

Geometric optics modeling

The tight focus geometry used in these experiments is shown in Fig. 1. To understand the effect of the temperature profile on the incoming light beam, Eq. (16) is expanded to the first order

$$n = n_0 + \Delta n_0 \left(1 - \frac{2r^2}{\omega^2}\right) \tag{17}$$

where for a temporally square pulse, of width τ, $< n_0(t) >= (H(\tau)\alpha/\rho c)(dn/dT)$. Due to the radial dependence of the refractive index, the sample will behave as a lens. This means that a ray matrix formulation may be employed to model the behavior of a laser pulse as it propagates through the system. Using Eikonal equation in the paraxial limit

$$\frac{d}{ds}\left(n\frac{d\vec{r}}{ds}\right) \cong \frac{d}{dz}\left(n\frac{d\vec{r}}{dz}\right) = \vec{\nabla} n \tag{18}$$

a medium of thickness L and a quadratic index profile of the form

$$n = n_0(1 - K^2 r^2/2) \tag{19}$$

can be represented by a ray matrix[17]

$$\begin{pmatrix} A & B \\ C & D \end{pmatrix} = \begin{pmatrix} cosKL & \frac{1}{K}\sin KL \\ -K\sin KL & \cos KL \end{pmatrix} \tag{20}$$

where L is the sample thickness and, from Eq. (12),

$$K = \sqrt{4\Delta n_0/(n_0 + \Delta n_0)\omega^2}. \tag{21}$$

Here ω is the beam radius at the sample. In the geometry shown in Fig. 1, the beam radius varies with position which means that the matrix in Eq. (14) must be continuously altered. However, for a thin sample ($L <<$ Rayleigh range), the
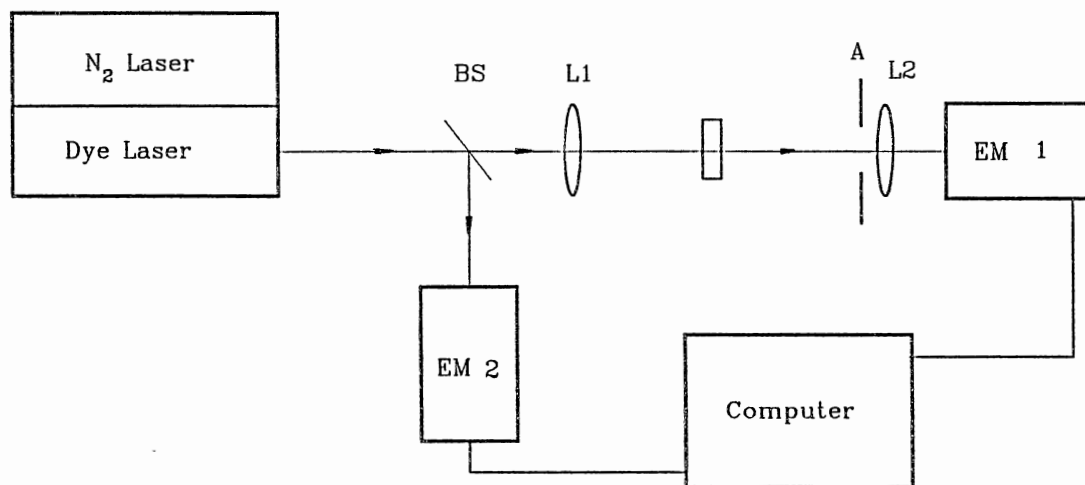
Figure 1. Experimental setup used for Z-scan and FT experiments. M is the distance from laser to lens 1 (L1)=325 cm, Z is the distance from L1 to the sample. EM is the energy meter.

beam radius along the medium can be assumed to be constant. Therefore, the ray matrix for the total propagation from the beam spot in the laser to the aperture is

$$
\begin{pmatrix} A & B \\ C & D \end{pmatrix} = \begin{pmatrix} 1 & Y \\ 0 & 1 \end{pmatrix} \begin{pmatrix} 1 & 0 \\ 0 & n_0 \end{pmatrix} \begin{pmatrix} \cos KL & \frac{1}{K}\sin KL \\ -K\sin KL & \cos KL \end{pmatrix}
$$
$$
\times \begin{pmatrix} 1 & 0 \\ 0 & \frac{1}{n_0} \end{pmatrix} \begin{pmatrix} 1 & Z \\ 0 & 1 \end{pmatrix} \begin{pmatrix} 1 & 0 \\ -\frac{1}{f} & 0 \end{pmatrix} \begin{pmatrix} 1 & M \\ 0 & 1 \end{pmatrix} \tag{22}
$$

where the parameters are given in Fig. 1. The complex beam radius, q(z), at the aperture can now be related to the complex beam radius at the beam spot in the laser via the ABCD law

$$
q_2 = \frac{Aq_1 + B}{Cq_1 + D} \tag{23}
$$

where

$$
\frac{1}{q(z)} = \frac{1}{R(z)} - i\frac{\lambda}{\pi\omega^2(z)} \tag{24}
$$

here $R(z)$ is the curvature of the beam. Thus the beam radius at the aperture for a thin sample can be analytically found to be

$$
\omega_f = \left(\frac{Z\lambda}{\pi\omega(Z)^2}\right)^2 + \omega(Z)^2\left(\frac{M}{Z} + \frac{4L\Delta n_0}{\omega(Z)^2}\right) \tag{25}
$$

This first order approximation to ω_f can be used to understand the relevance of some of the experimental parameters. Since the fractional power transmitted through an aperture of radius "a" is given by

$$
T = \int_0^a P(r)2\pi r \, dr = 1 - e^{-\frac{2a^2}{\omega_f^2}} \tag{26}
$$

the energy at the detector is proportional to $\exp{(-\alpha L)}[1 - \exp{(-2a^2/\omega_f^2)}]$, where ω_f is the beam radius at the aperture. Therefore, to minimize the output fluence, ω_f must be maximized.

Effects of experimental parameters

The parameters involved in the FT experiments can be divided into two categories: geometric and material. The first includes parameters such as sample position, sample thickness, and beam radius at the sample, while the second includes parameters such as the thermo-optic coefficient, specific heat capacity, linear coefficient of thermal expansion, and absorption coefficient. The effects of these parameters are considered for a *"thick"* sample which is modeled as a stack of thin samples through which the beam radius remains constant. The iteration is done using a computer model which calculates the beam waist at the front surface of a slice and propagates the beam through it after formation of the proper matrix elements.

The importance of the sample location in an FT experiment was known as early as[5] 1977 and its optimization is found from results of a Z-scan[18] experiment. For a fixed input energy, transmittance at the aperture is calculated as a function of the sample position, Z, measured from L1. A plot of such a calculation is shown in Fig. 2. For the subsequent analysis, the sample is placed at the minimum transmittance of the Z-scan, point 1 for $dn/dT > 0$ or point 2 for $dn/dT < 0$. For the sample positioned as described above, the energy at the detector is plotted versus input power for various values of dn/dT in Fig. 3. For a given dn/dT, at high input powers, the deviation from a linear optical response causes a clamping effect in the fluence transmitted through the aperture with two important characteristics. First, the clamped fluence decreases with an increase in the absolute magnitude of dn/dT. This is to be expected from the direct relationship between the change in the index of refraction and dn/dT as seen in Eq. (10). Second, for a given magnitude of dn/dT, the clamped output fluence is lower for a positive dn/dT. The cause of this asymmetry in output fluence can be better understood if the sample is viewed as a series of stacked positive lenses for $dn/dT > 0$ or negative lenses for $dn/dT < 0$. For the case of $dn/dT > 0$, the
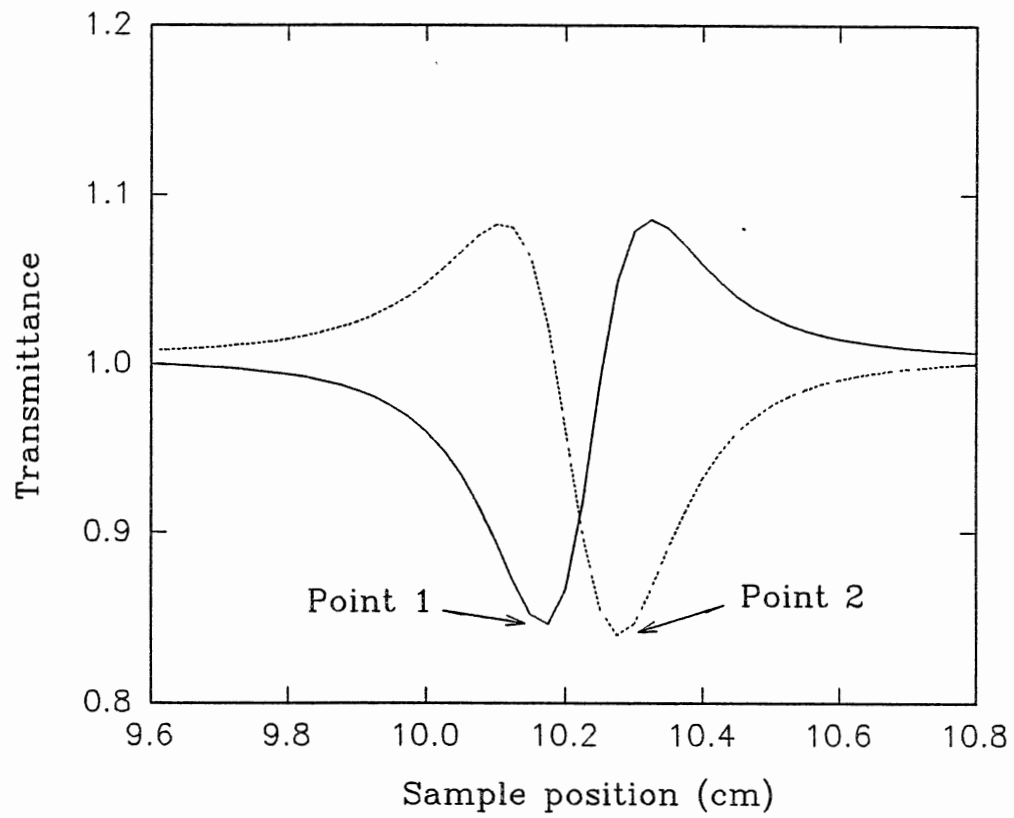
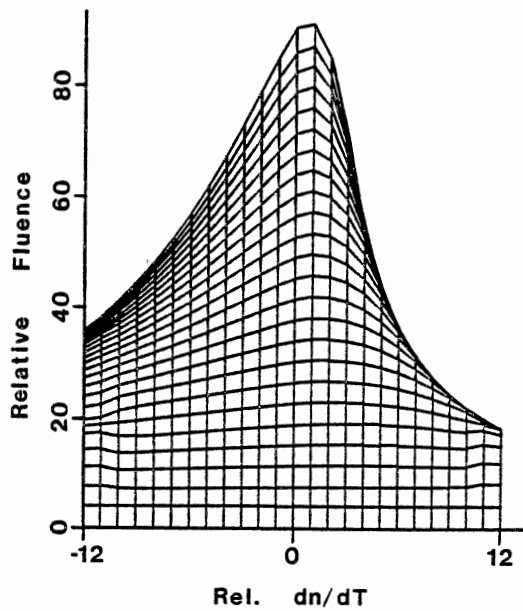Figure 2. Normalized transmittance vs sample distance from L1 for $dn/dT > 0$ (solid) and $dn/dT < 0$ (dash).
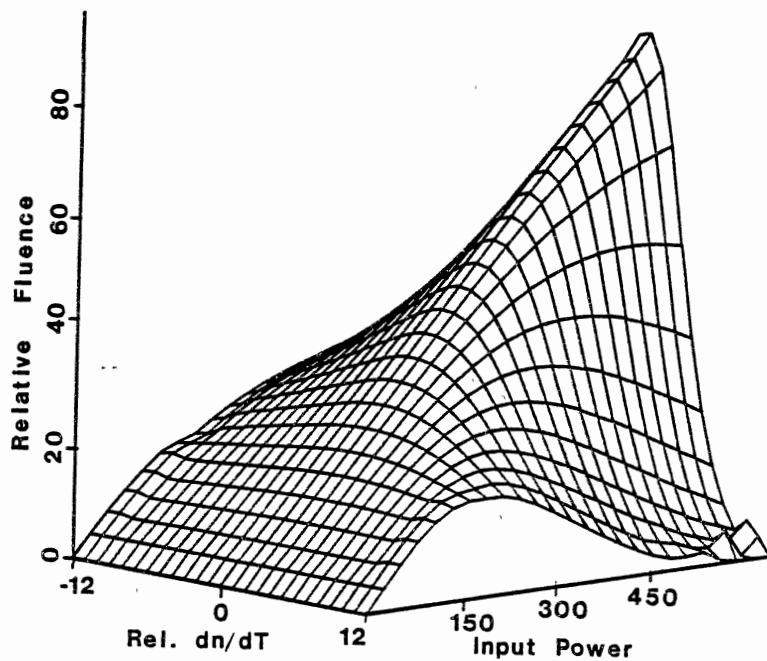
Figure 3. Transmitted fluence (z-axis) as a function of incident power for various values of dn/dT: (a) viewed at 45^0 to the axis, (b) viewed perpendicular to the dn/dT axis.

back slices display an additional increase in their focusing power due to the presence of the front slices which focus the beam further. This translates into a lower transmittance at the aperture. For $dn/dT < 0$, however, the back slices undergo a decrease in their focusing power caused by the presence of the front slices which tend to defocus the beam further. Since lower clamping values are desired for many device applications[15,16] of thermal lensing, materials exhibiting $dn/dT > 0$ are preferable.

Since α and L appear as a product in Eq. (18), (αL) may be considered as one parameter. From Eq. (18), it is apparent that an increase in the absorption coefficient or sample thickness will induce a greater ω_f which in turn lowers the clamped fluence. An increase in either of these parameters, however, also reduces the throughput efficiency of the material in the linear response regime. In some glasses the absorption coefficient is not a constant with input power. In these nonlinear optical materials, the analysis presented above has to be modified to account for this property. Figure 4 is the plot of the Z-scan and FT results obtained in the presence of an intensity dependent optical absorption coefficient of the form

$$\alpha = \alpha_0 + \beta I. \tag{27}$$

Figure 4b shows that a decrease in the clamped output occurs with an increase in the nonlinear optical absorption coefficient.

A direct interpretation of the remaining parameters in Eq. (13), ρ and c, reveals that a low density and specific heat cause an increase in the thermal lensing response of the material. This is expected, since for a low ρc a greater increase in the temperature of the sample occurs for a given input energy ($\Delta Q \sim \rho c \Delta T$).
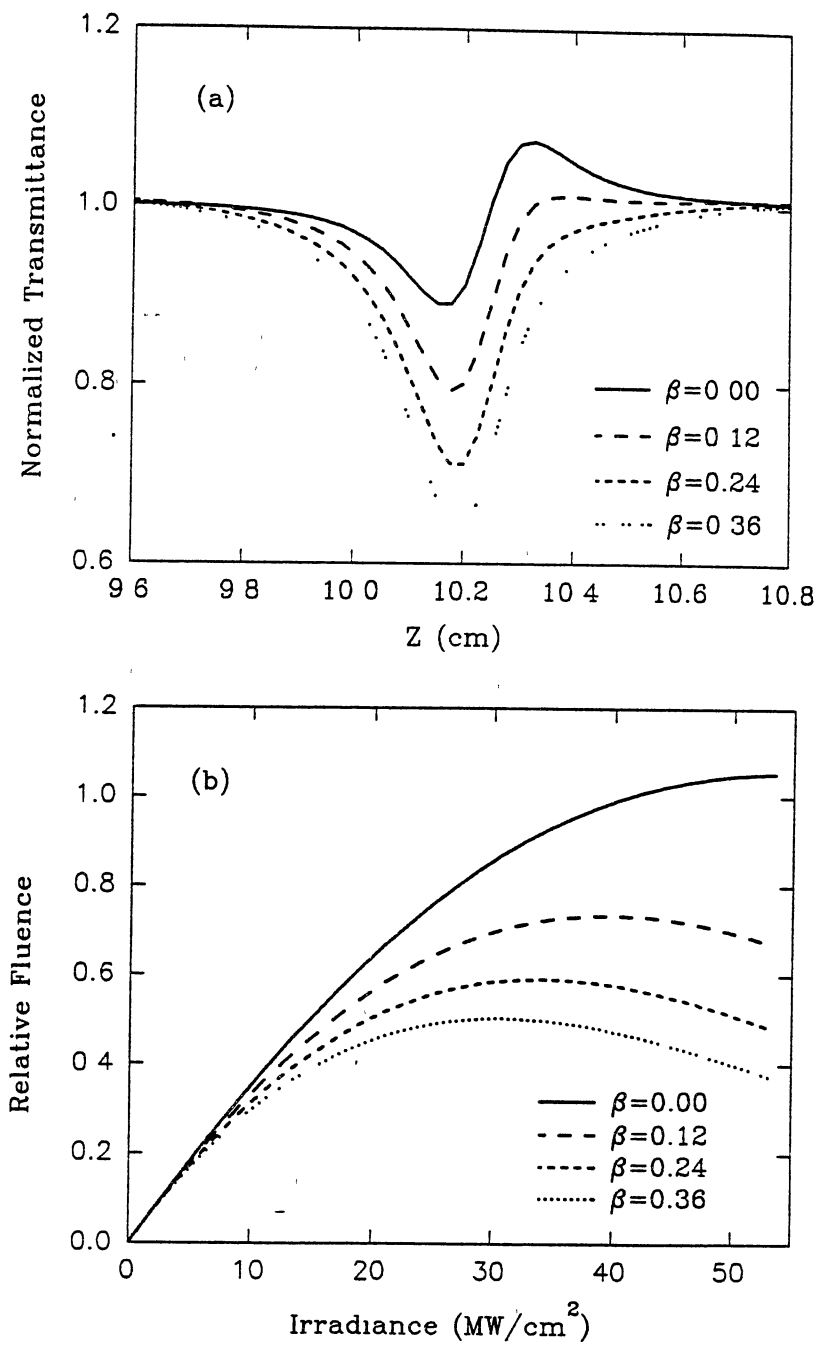
Figure 4. Effects of nonlinear absorption on the thermal lensing behavior in (a) Z-scan and (b) FT experiments for various values of β (cm/MW). $\gamma = 15 \times 10^{-13}$.

CHAPTER III

EXPERIMENTAL

Experimental setup

A 300 kW peak power nitrogen laser was used to pump Coumarin 460 dye to obtain 7 ns pulses at 457 nm. The beam was passed through an attenuator and was focused by a 10 cm focal length lens (L1). It was then recolumnated by second lens (L2) after passing through the sample and an iris diaphram (aperture "A"). To monitor the incident energy on the sample, a beam splitter, BS, reflected 5% of the beam onto a Precision Tech energy meter. At sufficiently high input irradiance (few MW/cm2), the optical nonlinearity of the material caused the beam to fan out, thereby decreasing the transmitted energy through the aperture. Measuring the transmitted fluence as a function of input intensity is referred to as a fluence transmission (FT) experiment. The radius of the aperture is an important variable and was set so that 90% of the incoming energy was incident on the energy meter, EM 1, at low irradiances. The location of the sample with respect to the focal plane of lens 1 is an important parameter.[18] In the experiments described below, the sample was first moved with respect to the focal plane of lens 1 while measuring the transmitted energy. This is referred to as a Z-scan experiment. The sample was then located at the position yielding the lowest transmitted energy through the aperture for high input irradiance, and FT experiments are performed while the input irradiance is varied in the range 0 - 20 MW/cm2.

Effect of parameters

Using the geometry described earlier, the fluence transmission was measured for different input irradiances. Figure 5(a) is the plot of the output fluence,

averaged over 10 pulses, for various input irradiance for sample LS1. The output fluence followed curve "a" until point 1 where a transition from point 1 to point 2 was observed. The behavior was then dictated by curve "b". The nonreversibility of the process suggests the occurrence of optical damage. Examination with an optical microscope revealed the presence of surface damage. It was found that the damage threshold was increased with application of a thin layer of refractive index matching fluid to the front surface of the sample. Figure 5(b) is a photograph of the surface of the LS1 glass exposed to intensities greater than the damage threshold. It is seen that application of index matching fluid reduces increases the damage threshold.

To study the fluence transmission without the effect of surface damage, the sample was translated in the x-y plane after each pulse. Figure 6 is a plot of the Z-scan, and fluence transmission results obtained using single shots on unirradiated surface areas. The solid line is the theoretical fit to the data using the parameters stated in Table II and the iteration process described earlier. From the Z-scan data, it was apparent that the glass exhibited a nonlinearity in the absorption coefficient. FT experiments with a fully opened aperture were used to investigate this behavior. Using Eq. (29) and a least squares fit to the data in Fig. 7, a value of 0.35 (cm/MW) was estimated for β. The origin of this nonlinearity (two-photon absorption, etc.) could not be determined from these results since FT experiments could not be extended to high enough input irradiances to accurately identify the exponent of the intensity dependence.

To elucidate the effect of sample thickness on the FT curve, experiments were performed on a 1.5 mm thick sample of 35% lead silicate glass and the results are compared to those obtained on the 1 mm thick sample (LS1) in Fig. 8. The triangles are the data for the 1 mm thick sample, normalized for thickness variations such that in the linear transmission region both glasses follow the same FT curve. As discussed earlier, α and L appear together. Therefore, it can be concluded that an increase in the absorption coefficient and/or an increase in the
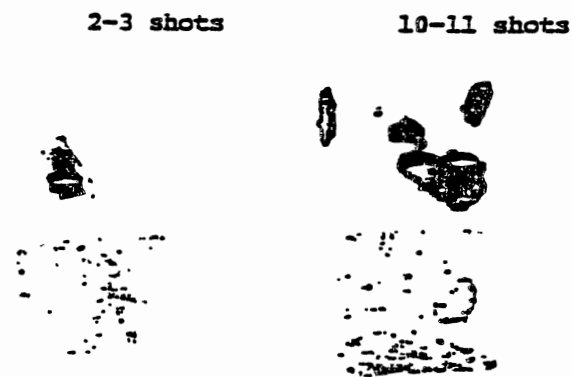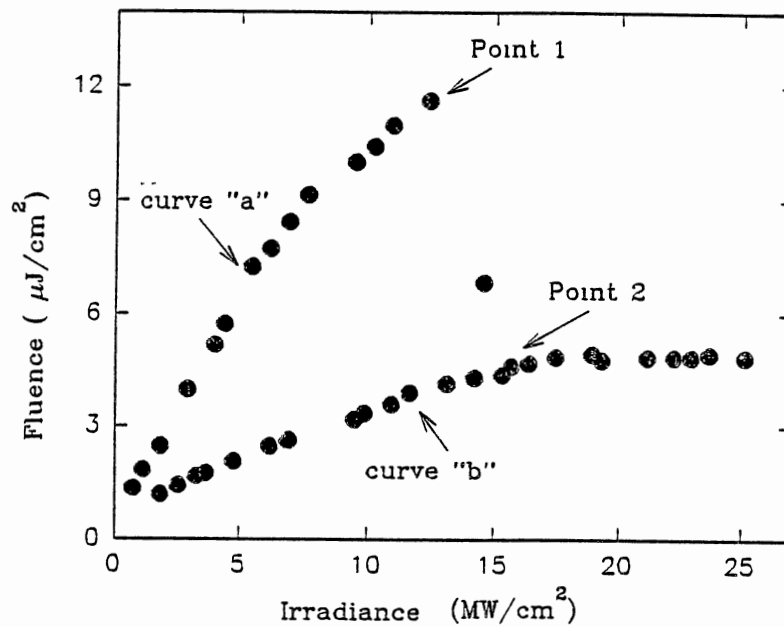
Figure 5. Surface damage characterisics of LS1 glass in FT experiments (a) point 1 is indicative of surface damage (b) increase of damage threshold via use of index matching fluid.
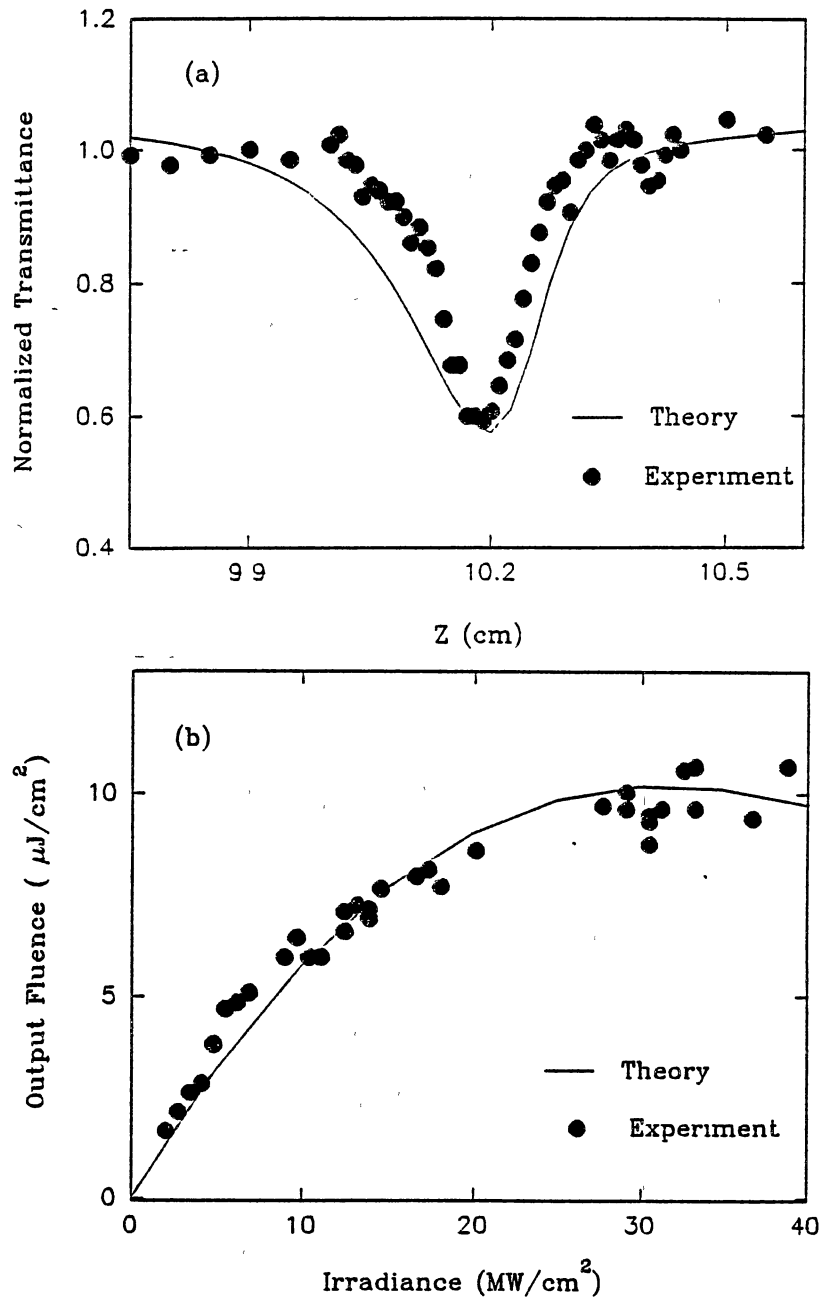
Figure 6. (a) Z-scan and (b) FT results of LS1 glass under a single-pulse geometry. The solid line is the theoretical fit to the data.
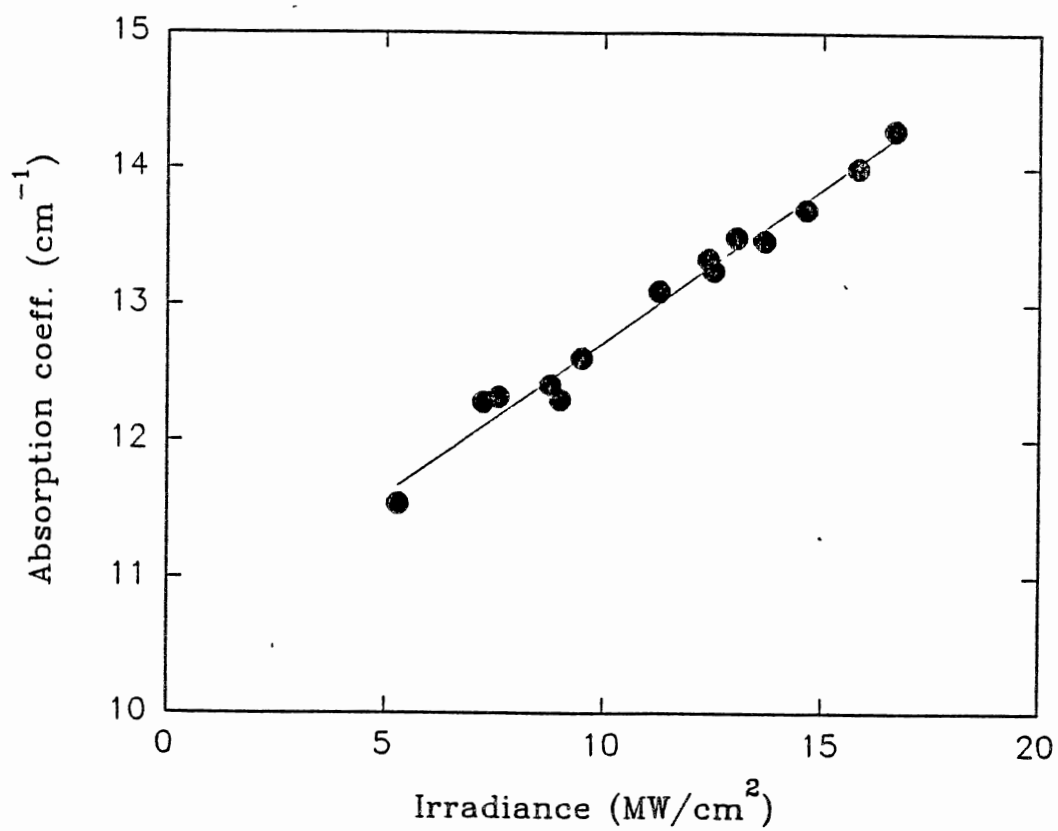
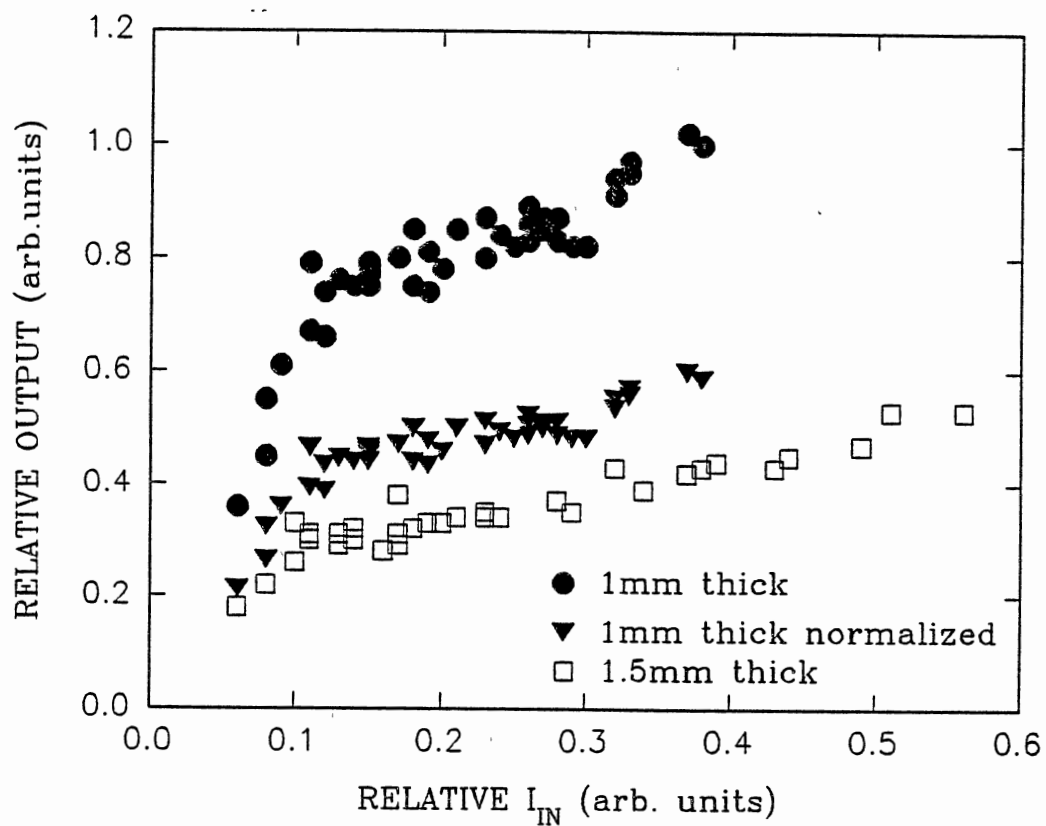Figure 7.   Intensity dependence of the absorption coefficient of LS1 using $\alpha = \alpha_0 + \beta I$.

Figure 8. Thickness dependence of the FT experiments. The triangles are the results of the 1 mm thick LS1 glass normalized for the difference in the absorption of light in the linear regime.

thickness of the material will result in a decrease in the clamped fluence level of the output.

Effects of lead concentration on the thermal lensing properties of these glasses were studied by performing FT experiments on the LS2 glass. The results are compared to those obtained on the LS1 glass in Fig. 9. As before, the plots are normalized for the differences in the absorption coefficients and thicknesses of the glasses. It is observed that an increase in the lead concentration from 24% to 35% results in a decrease in the clamped output fluence. To investigate the role of the glass network former ions, Z-scan and FT experiments were performed on a number of the glasses with different compositions. Figure 10 shows the results obtained for the lead glasses that are listed in Table I. It is apparent that the network formers play an important role in the thermal properties of lead glasses. In particular, it is seen that the clamped output fluence of the germanate and silicate glasses are lower than those of the borate and phosphate glasses.
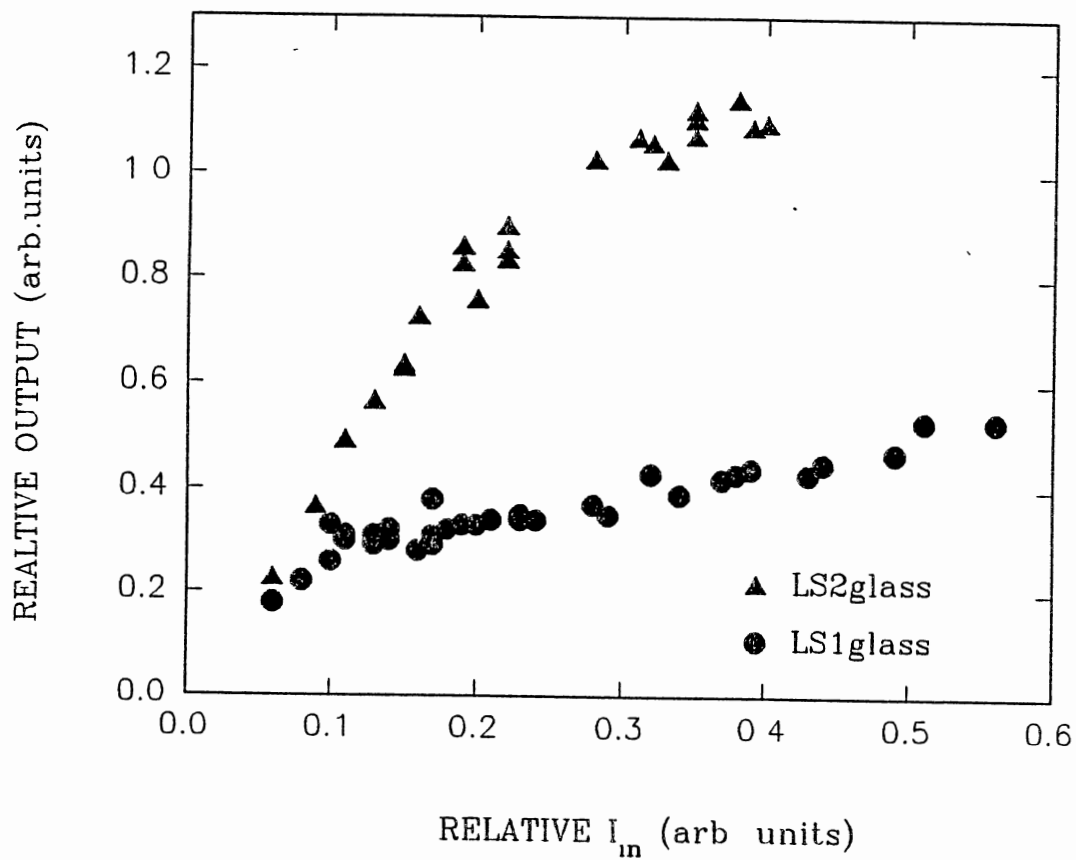
Figure 9. Effect of the lead concentration on the output of FT experiment. The data is corrected for the difference in the absorption coefficient in the linear regime.
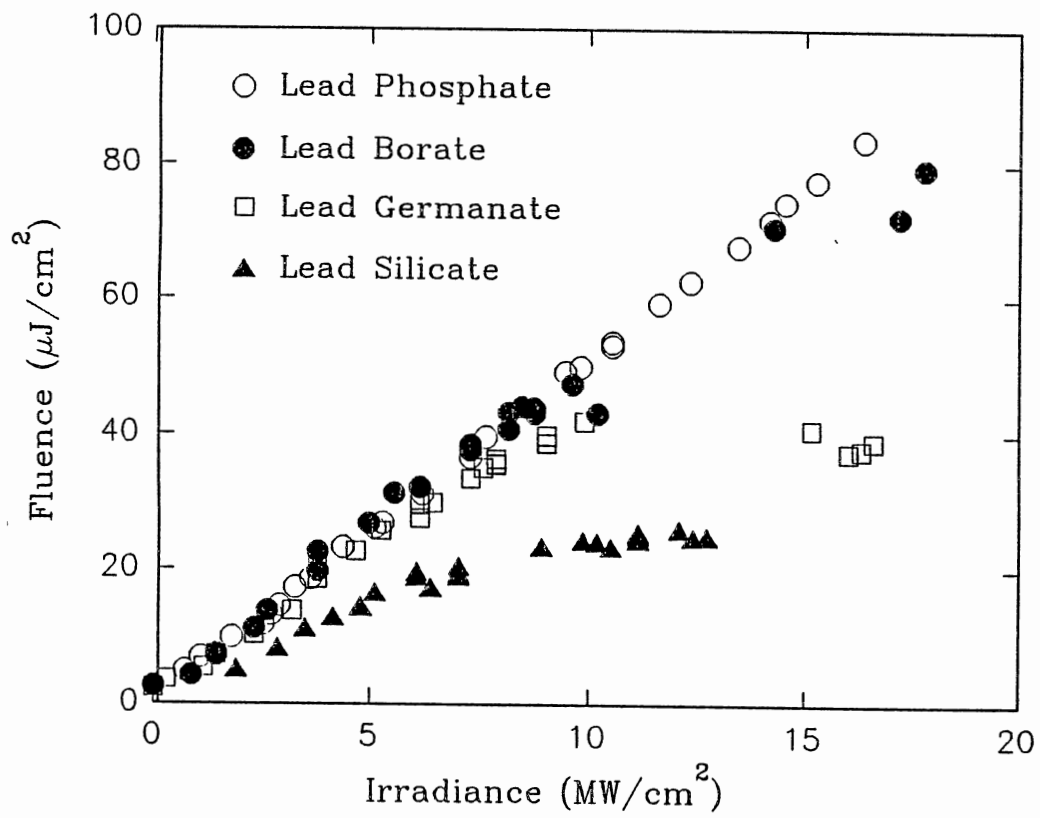
Figure 10. Results of the FT experiments on lead glasses with different network former.

CHAPTER IV

DISCUSSION

Table II is a summary of the results obtained for the glasses studied. The nonlinear coefficients γ and b were determined from a computer fit to the FT and Z-scan data using the measured beam radius of 50 μm at the front surface of the sample. An order of magnitude estimate for (ρc) of the glasses was found by direct measurement of the temperature increase of an aluminum container of water due to insertion of a pre-heated sample,

$$(mc\Delta T)_{glass} = (m_w c_w + m_{Al} c_{Al}) \, \Delta T_w. \tag{28}$$

There is some degree of uncertainty in the exact values obtained by this technique due to the approximate nature of the theoretical model and calorimetric measurements. However, these values are useful in comparing the relative thermal lensing properties of different glasses. The order of magnitude of the values obtained for dn/dT is consistent with typical values reported in the literature for lead glasses[8]. This indicates that the main contribution to the change in the optical path length in Eq. (10) in these glasses is due to the thermal change in the refractive index. As stated earlier, in some laser glasses such as phosphates[14], the main contribution to lensing arises form the second term in Eq. (10).

Due to the thermal nature of the nonlinearity of interest here, material parameters such as the absorption coefficient and heat capacity play an important role in determining the magnitude of the thermal lensing in a specific material. The nonlinear process is directly associated with the parameters dn/dT and β. It is necessary, therefore, to understand the effects of the network former and modifier ions in determining the magnitude of these parameters.

TABLE II

MATERIAL PARAMETERS

Glass	γ $(10^{-13} cm^2/W)$	β (cm/MW)	α (cm^{-1})	ρc (cal/Kcm^3)	dn/dT $(10^{-5} K^{-1})$
LS1	3.0	0.35	10.47	0.9	1.5
LS2	3.0	0.12	3.15	0.7	4
LG	2.4	0.12	2.54	1.3	7
LB	0.2-0.6	<0.05	1.20	0.9	0.8-2
LP	<0.3	<0.05	1.34	0.9	<0.9

Lead glasses were found to have strong thermal lensing properties. This is attributed to the increase in the absorption coefficient of the glasses at 457 nm due to the presence of lead as a modifier ion. Furthermore, from the results obtained for samples LS1 and LS2 it can be concluded that a greater ratio of PbO/SiO2 will result in an increase in the nonlinear absorption coefficient. It should be noted that the nonlinearity in the absorption coefficient is not solely dictated by the presence of lead since LP and LB glasses, which contain the same concentration of lead as LS2 and LG glasses, have much smaller nonlinear absorption coefficients.

From typical values for the linear thermal expansion coefficients of similar materials[19] ($\zeta_{Germanates} > \zeta_{Silicates} \sim \zeta_{Phosphates} \sim 2\zeta_{Borates}$) and the results shown in Table II, it can be concluded that during excitation with pulses of 10 ns in duration: (i) the main contribution to the thermo-optic coefficient arises from the first term in Eq. (11) (i.e. a change in the electronic polarizability of the glass components with temperature), and (ii) the network former ions play an important role in determining the magnitude of dn/dT. Since in dielectric materials the electronic polarizability of an atom is caused by a slight displacement of the negatively charged electron clouds relative to the positively charged nucleus, and in a classical picture the electron is bounded harmonically to an atom, it is apparent that the electronic polarizability of a material should decrease with an increase in the charge-to- radius ratio of the ions. Oxygen ions are highly polarizable due to their charge-to-radius ratio. Due to their high concentration in the glasses studied, the change in the polarizability of O^{2-} ions makes the dominant contribution to the thermal lensing properties. The strength of the polarizability change is effected by the glass structure through the electronic polarizing power[10] (Q/r^2) of the network former ions. The greater Q/r^2 ratio of the silicates to that of the germanates can be used to explain the greater thermo-optic coefficient of germanates since, as stated earlier, an increase in the Q/r^2 ratio of the network former restricts changes in the electronic polarizability of the oxygen ions. This model can be extended to include other glasses lacking oxygen such as fluoride glasses. In these glasses the relatively small polarizability[20], Φ, of the F^- ions

and a large thermal expansion coefficient[19], ζ, results in $dn/dT < 0$ for these glasses.

In addition, for the glasses studied, the results show that the strongest thermal lensing effects are found in random network structures of silicates and germanates compared to the chain- or ring-type network structures of the phosphate and borate glasses. This is due to the greater degrees of freedom available to the oxygens in the less constrained random network structures not available to the chain-type structure of the phosphates, containing P=O bonds, or the ring-type structure of borates which strongly limit the cross linking ability of the oxygens.

In summary, effects of the geometrical and material parameters on FT experiments were studied for glasses with a variety of compositions using a tight focus geometry. It was found that lead silicate glasses exhibited the greatest thermal lensing properties of the glasses investigated with the results varying with glass structure and lead concentration. In conclusion, to maximize thermal lensing in this type of experiment, glass materials should have high values of αL, small values of ρc, a random network structure with a maximum number of degrees of freedom and a high polarizing power, network modifier ions with high polarizability, and a high threshold for optical damage of the surface. With these criteria in mind, it should be possible to produce a glass with significantly enhanced thermal lensing properties and design methods for protecting against surface damage.

CHAPTER V

DEVICE APPLICATION

Optical limiting

With the development of high power lasers the demand for passive beam control has increased dramatically. Currently, this is achieved via optical limiters which clamp the output beam through them above a certain threshold. Figure 11 shows the response of an ideal limiter. In the linear region, the sample is transparent to the incident beam. At a certain threshold, I_T, the output of the device will remain constant. Optical limiters are the optical analogy to current limiters and as such may be employed, in the future, as a component of optical processing. Current use of these devices is limited to the sensor and eye protection which utilize the nonlinearites of materials and therefore need material with high nonlinearity.

Optical limiting can be achieved via free carrier absorption semiconductors. Limiting in these materials is caused by absorption of the free carriers which have been promoted to the conduction band via two photon absorption. These devices have high damage threshold and are suited for fast pulse limiting (Picoseconds). However, the threshold for limiting is dictated by the two photon absorption coefficient and is thus higher than the damage threshold of most of the materials that is designed to protect.

From the results obtained in the above chapters, it can be concluded that thermal lensing can be utilized as an optical limiting device. In addition to its low clamping intensity, and the workability of glasses, glasses exhibit absorption across the whole visible spectrum. This means that they are ideal for limiting the input intensities to eyes. With this in mind, the setup described in Fig.1 can be used
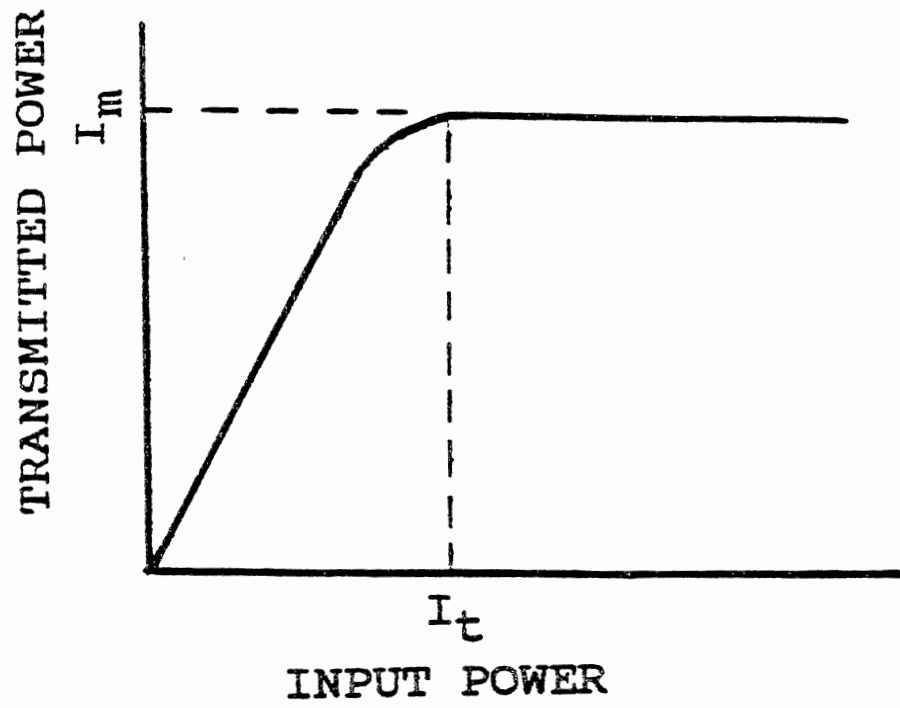
Figure 11. Behavior of an ideal limiter.

to describe the limiting abilities of these glasses as eye protection devices. The damage threshold for permanent eye damage occurs at $0.3\mu J/cm^2$. Lead silicate has a clamping fluence of $10\mu J/cm^2$. Though this is not sufficient, it does indicate the usability of thermal lensing for optical limiting.

Since the damage threshold for eye is wavelength independent the limiter must function in the whole visible spectrum. This is the greatest downfall of these devices, since both dn/dT and α are wavelength dependent quantities. This means that research needs to focus on increasing the response of the materials throughout the spetrum. This is achieved by (i) modification and optimization of the present geometry, (ii) imporvement of the existing materials as well as use of new materials.

The optimization of the tigth focus geometry was investigated earlier in this thesis. It was shown that in the absence of nonlinear absorption, the optimum sample positions for $dn/dT > 0$ differed from $dn/dT < 0$. This suggests the possibility of using two samples in the same experiment, one with $dn/dT < 0$ and the other with $dn/dT > 0$. This effect was investigated using the computer model presented in Chapt.II. Figure 12 shows the Z-scan resulting form the presence of two samples in the tight focus geometry. Two important characteristics can be attained form these figures. Firstly, a shift in the optimum sample positions is observed. This can be attributed to the fact that the presence of the second sample alters the position of the focal point. Secondly, positioning of the second sample in the valley of its Z-scan resulted in enhancement of the nonlinearity of the first sample. In Figs. 12 (a) and (b) line 1 indicates the Z-scan in the absence of the second sample and line 2 indicates the Z-scan with the second sample placed in its optimum position (valley of its Z-scan). Though no experimental results have been obtained for this result, it can be utilized in the future to increase the dynamic range of these devices. A more direct approach to the decrease of the clamping fluence involves modification of the existing materials and investigation of the new materials.

With this in mind, a 1 cm^2 region of LS1 sample was exposed to IR radiation from a 10 ns pulsed Nd:YAG laser operating at 1.06 μm prior to an FT
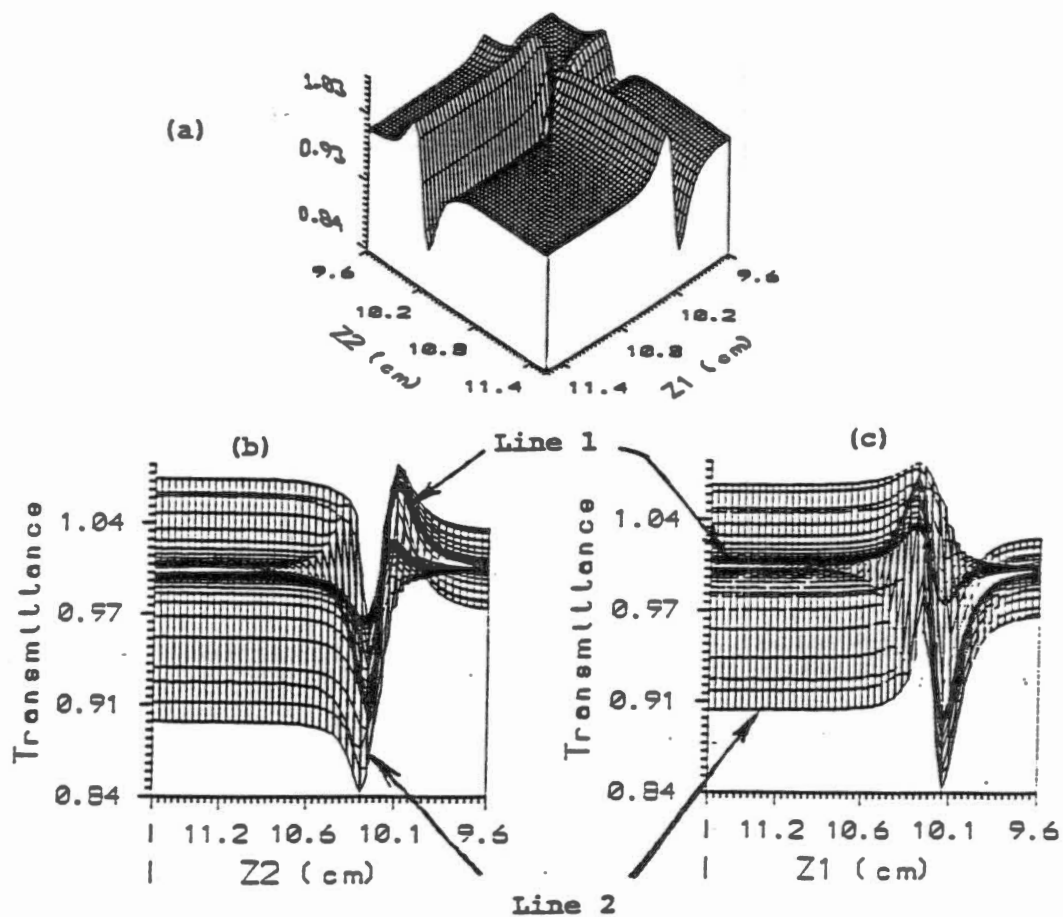
Figure 12. Optimization of 2 sample Z-scan. $dn/dT > 0$ for sample 1 and $dn/dT < 0$ for sample 2. In (b) and (c) line 1 is the Z-scan results in the absence of the second sample

experiment. This resulted in a lowering threshold intensity and thereby a lowered clamped fluence. Figure 13 is the plot of the FT experiments for the IR radiated and the unirradiated samples. A change in the slope in the visible region is also apparent. Since the surface damage had not decreased, it can be concluded that the alteration in the optical properties had occurred in the bulk of the material. An absorption spectra of the sample taken with CARY 2400 shows a alteration in the absorption spectra of the glass in the visible region (Fig. 14). To further investigate this Phenomena, number and intensity of IR pulses incident on the sample were varied in a systematic way and FT experiments were performed on these regions. It was found that the clamping fluence was related to the number of incident pulses in a small extend. Figure 15 shows the FT results for LS1 samples which had been exposed to 10, 20 100 pulses of 50 MW peak power radiations. Experiments were then performed on regions which were exposed to various IR intensities. Figure 16 shows the clamped output dependence on the IR intensity. The variation of FT results with the number and intensity of incident pulses suggested an energy dependent phenomena. This was investigated using a diode pumped YAG laser operating in the continuous mode. FT experiments on this region showed no alteration in the material properties and thus it was concluded that the phenomena is intensity dependent. Though the cause of this change is not understood, the change can be used to modify the sample to be better suited as a limiter. The flattening of the absorption spectra will allow this glass to be used as a limiter in a wider region of spectrum and therefore this phenomena should be investigated further. The flattening of the absorption spectra can also be achived by introduction of other modifiers with absorption in the higher wave lengths. This phenomina is currently being investigated by introduction of iron in the glasses used.

Lastly, new materials such as lead bismuth and lead galate glasses show great promise since the show a greater transmittivity in the linear region and a low clamping in the nonlinear region. Figure 17 is the FT results of lead bismuth glass in the same configuration described earlier.
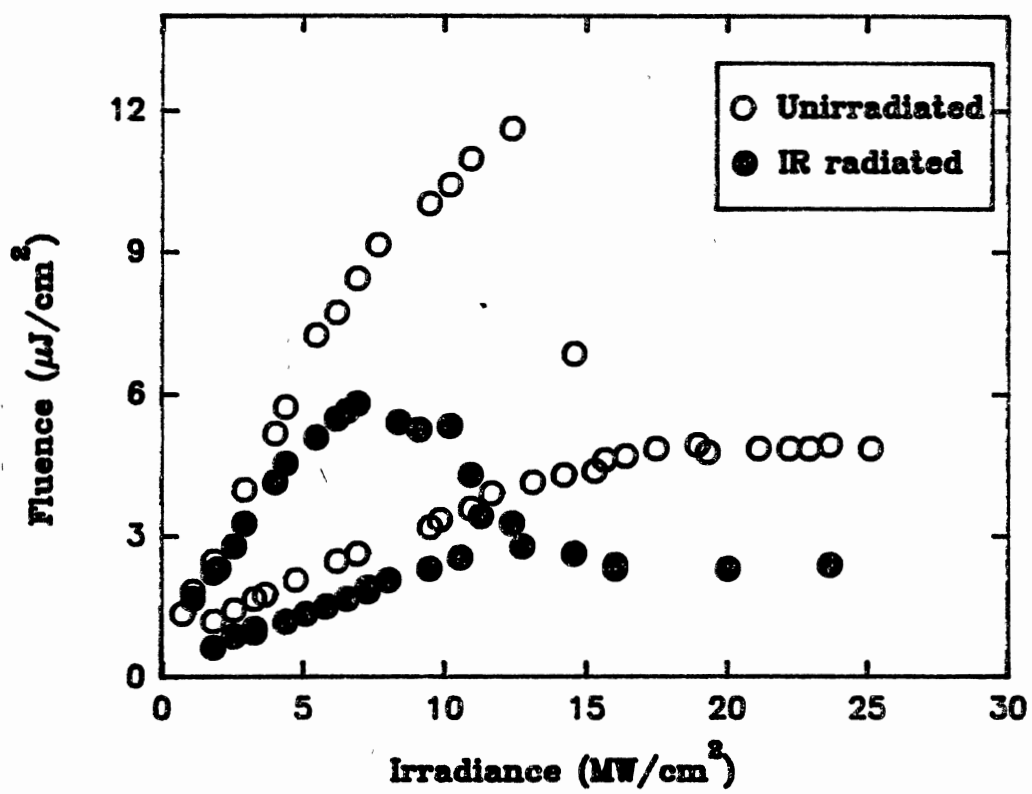
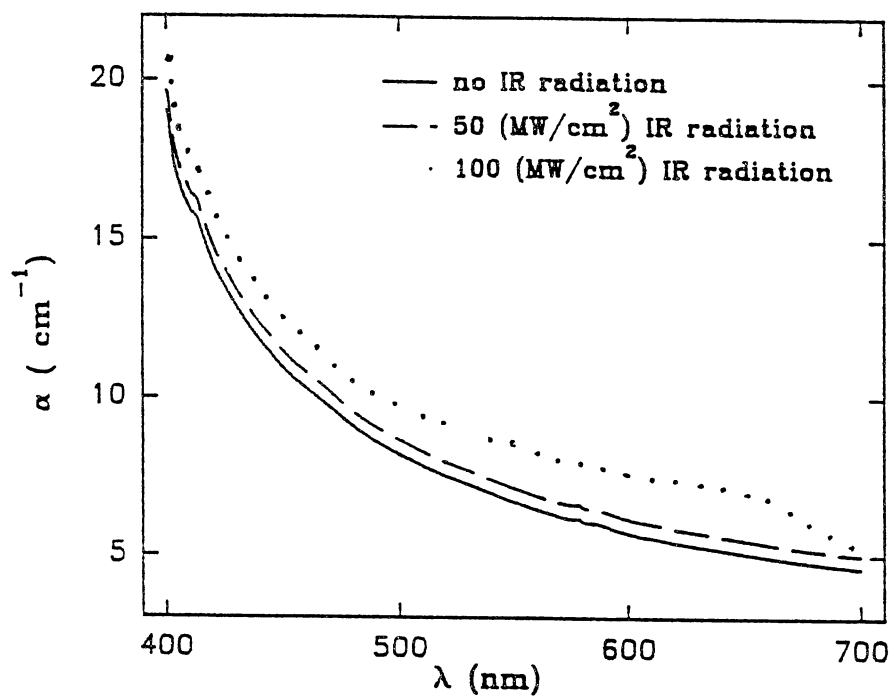Figure 13. Effects of IR radiation on the FT experiment.

Figure 14. Effects of IR radiation on the absorption spectra of LS1 glass.
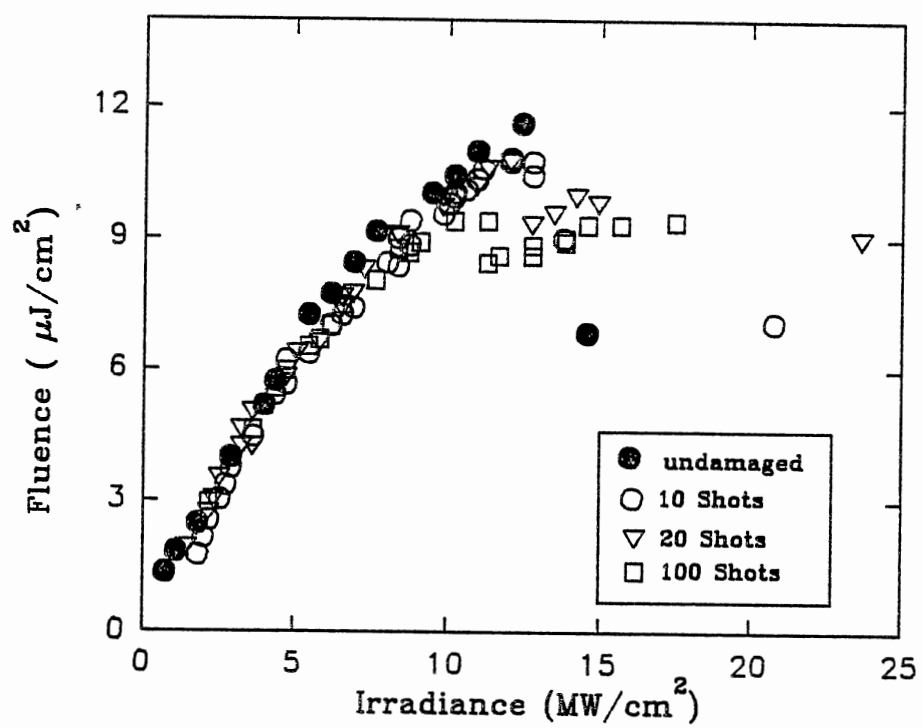
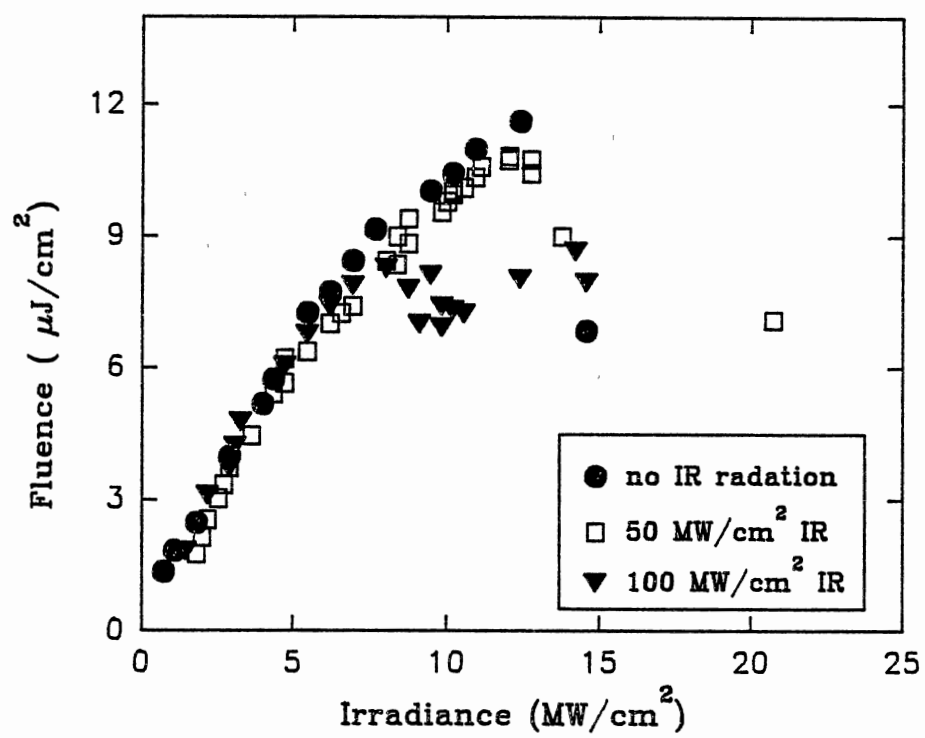Figure 15. Effect of Nd:YAG repetition rate on the FT results.

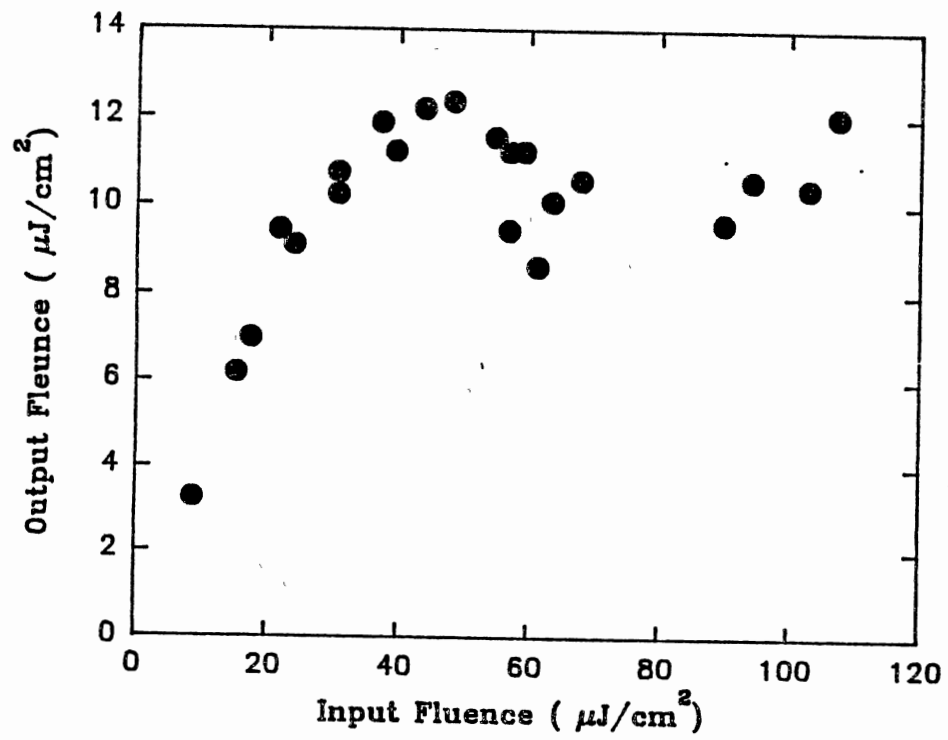Figure 16. Effect of IR peak power on the FT results.

Figure 17. Limiting characteristics of lead bismuth glass.

BIBLIOGRAPHY

1. A. Feldman, D. Horowitz, and R.M. Waxler; *IEEE J. Quant. Electr.* **QE-9**, . 1054 (1973).

2. S.A. Akhmanov, R.V. Khokhlov, and A.P. Sukhorrukov, " Laser Handbook", Ch. E3, (North-Holland, Amsterdam, 1972) p. 1151.

3. W.D. St.John, B.Taheri, J.P. Wicksted, R.C. Powell, D.H. Blackburn and D.C. Cranmer; *J. Opt. Soc. Am. B* **9**, 610 (1992).

4. J.H. Marburger; *Prog. Quant. Elect.* **4**, 35 (1975).

5. A.J. Twarowski and D.S. Kliger; *Chem. Phys.* **20**, 253 (1977).

6. M. Sparks; *J. Appl. Phys.* **42**, 5029 (1971).

7. E.P. Riedel and G.D. Baldwin; *J. Appl. Phys.* **38**, 2720 (1967).

8. J.P. Gordon, R.C.C. Leite, R.S. More, S.P.S. Porto, and J.R. Whinnery; *J. Appl. Phys.* **36**, 3 (1965).

9. F.W. Dabby, and J.R. Whinnery; *Appl. Phys. Lett.* **13**, 284 (1968).

10. T. Izumitani and H. Toratani; *J. Non. Cryst. Solids* **40**, 611 (1980).

11. G.D. Baldwin and E.P. Riedel; *J. Appl. Phys.* **38**, 2726 (1967).

12. R. Adair, L.L. Chase and S.A. Payne; *J. Opt. Soc. Am. B.* **4**, 875 (1987).

13. J.M. Jewell, C. Askins and I.D. Aggarwal; to be published in Proc. SPIE 1441.

14. M.M. Bubnov, A.B. Grudinin, E.M. Dianov, and A.M. Prokhorov; *Sov. J. Quantum Electron.* **8**, 275 (1978).

15. G.L. Wood, W.W. Clark III, M.J. Miller, G.J. Salamo, and E.J. Sharp; *SPIE Proceeding* **1105**, 154 (1989).

16. G.L. Wood, W.W. Clark III, and E.J. Sharp; *SPIE Proceedings* **1307**, 376 (1990).

17. A. Yariv; "Quantum Electronics", (John Wiley & Sons, New York, 1989).

18. M. Sheik-Bahae, A.A. Said, and E.W. VanStryland; *Opt. Lett.***14**, 955 (1989).

19. " Thermophysical properties of Matter Series",**13**, Y.S. Touloukian and E. H. Buyco eds., (Plenum, New York, 1977).

20. C. Kittel; "Introduction to Solid State Physics", (John Wiley & Sons, New York, 1986).

VITA

BAHMAN TAHERI

Candidate for the Degree of

Master of Science

Thesis: EFFECTS OF STRUCTURE AND COMPOSITION OF LEAD
GLASSES ON THERMAL LENSING

Major Field: Physics

Biographical:

Personal Data: Born in Tehran, Iran, September 3, 1965, the son of Ferei-
doun and Mehry Taheri.

Education: Received Bachelor of Science degree in Physics from California
Polytechnic State University, San Luis Obispo, California, June, 1989;
completed the requirements for the Master of Science Degree at the
Oklahoma State University, Stillwater, Oklahoma, July, 1992.